Available online at www.sciencedirect.com

ScienceDirect

Physics Procedia 3 (2010) 1279–1285

Physics Procedia

www.elsevier.com/locate/procedia

Graphene Energy Loss Spectroscopy: Perpendicular Case

Vassilios Fessatidis[a*], Norman J. M. Horing[b] and Makoto Sawamura[c]

[a]Department of Physics, Fordham University, Bronx, New York 10458, USA

[b]Department of Physics and Engineering Physics, Stevens Institute of Technology, Hoboken, New Jersey 07030, USA

[c]MANA, National Institute for Materials Science, Namiki, Tsukuba, Ibaraki, 305-0044, Japan

The energy loss of a fast charged particle probe incident on a two-dimensional graphene sheet is examined here. The fast particle motion is taken to be perpendicular to the $2D$ graphene sheet, which is considered to be in the degenerate limit of zero temperature. The response dynamics of the $2D$ graphene layer are described in the random phase approximation and the energy loss for particle motion perpendicular to the $2D$ graphene layer is calculated as a function of the velocity of the charged particle.

1. Introduction

The remarkable conduction properties of graphene have inspired intense and widespread research on its unusual properties. It is of interest to study its response to all probes, and in this paper we examine fast particle energy loss spectroscopy for graphene in the perpendicular case.

We analyze fast particle energy loss in terms of the effective potential $V(1)$ at space-time point $1 = (\mathbf{r}_1; t_1)$ induced by the Coulomb potential it impresses,

$$U(2) = \frac{Ze}{[\mathbf{r}_2 - \mathbf{R}(t_2)]}, \tag{1}$$

at space-time point $2 = (\mathbf{r}_2; t_2)$, polarizing the $2D$ graphene sheet. The frictional energy loss is assumed to be small, so that the motion of the charged particle is approximately uniform, i.e.,

$$\mathbf{R}(t_2) = \mathbf{v}t_2 + \mathbf{R}_0, \tag{2}$$

where $\mathbf{R}_0$ is the initial position vector of the charged particle.

The impressed potential, U, which is dynamically screened by the polarized graphene sheet (lying on the xy-plane), is characterized by an inverse dielectric function $K(1,2)$ describing its nonlocal relation to the effective potential, V, through

$$V(1) = \int d^4 2\, K(1,2)\, U(2)\,; \qquad K(1,2) = \frac{\delta V(1)}{\delta U(2)}, \tag{3}$$

*fessatidis@fordham.edu

doi:10.1016/j.phpro.2010.01.176

($d^4 2 = dr_2 dt_2$). This inverse dielectric function for the graphene sheet (in $3D$), $K(1,2)$, is related to the direct dielectric function, $\varepsilon(1,2)$, through

$$\int d^4 3 K(1,3)\,\varepsilon(3,2) = \int d^4 3 \varepsilon(1,3)\,K(3,2) = \delta^4(1-2)\,. \tag{4}$$

The induced charge density, ρ, associated with $V(1)$,

$$\rho(1) = \int d^4 3\, R(1,3)\,V(3) = \int d^4 3 \int d^4 4\, R(1,4)\,K(3,2)\,U(4)\,, \tag{5}$$

is described in terms of the density perturbation response function, $R(1,3) = \frac{\partial \rho(1)}{\partial V(3)}$ ("ring diagram"). Considering the contribution of the perturbed density to the effective potential, we have

$$V(1) = U(1) + \int d^4 3\, v_c(1-3)\,\rho(3)\,, \tag{6}$$

where

$$v_c(1-3) = \frac{e}{|\mathbf{r}_1 - \mathbf{r}_3|}\delta(t_1 - t_2)\,, \tag{7}$$

is the instantaneous inter-electron Coulomb interaction of the graphene plasma. Taking the variational derivative of Eq. (6) with respect to $U(2)$ and using the chain rule of variational differentiation, we have

$$K(1,2) = \delta^4(1-2) - \int d^4 4\, \alpha(1,4)\,K(4,2)\,, \tag{8}$$

where $\alpha(1,2)$ is the polarizability, which will be written in a form that describes both the free electron response and an additive static background term $\alpha_0 = \varepsilon_0 - 1$ (ε_0 is the background dielectric constant) as

$$\begin{aligned} \alpha(1,2) \;&= -\int d^4 3\, v_c(1-3)\,R(3,2) + \alpha_0 \delta^4(1-2) \\ &= \varepsilon(1,2) - \delta^4(1-2)\,. \end{aligned} \tag{9}$$

Combining Eqs. (8) and (9), we obtain an integral equation for $K(1,2)$,

$$K(1,2) = \frac{1}{\varepsilon_0}\delta^4(1-2) + \frac{1}{\varepsilon_0}\int d^4 4 \int d^4 3 v_c(1-3)\,R(3,4)\,K(4,2)\,.$$

Applying the operator ∇_1^2 to the above equation, we get

$$\nabla_1^2 \left[K(1,2) - \frac{1}{\varepsilon_0}\delta^4(1-2) \right] = -\frac{4\pi e}{\varepsilon_0} \int d^4 4 R(1,4)\,K(4,2)\,. \tag{10}$$

Comparing Eqs. (5) and (10), we obtain the perturbed density, $\rho\,(1)$, as

$$\rho(1) = -\frac{\varepsilon_0}{4\pi e} \int d^4 2\, \nabla_1^2 \left[K(1,2) - \frac{1}{\varepsilon_0}\delta^4(1-2) \right] U(2)\,. \tag{11}$$

The force per unit volume on the electron plasma due to the passing charged particle is $-\rho(1)\,\nabla_1 V(1)$ and the reaction force on the fast particle is

$$\mathbf{f} = e\int d^3\mathbf{r}_1\rho(1)\,\nabla_1 V(1) = -\frac{\varepsilon_0}{4\pi}\int d^3\mathbf{r}_1\,\nabla_1^2\left[V(1)-\frac{1}{\varepsilon_0}U(1)\right]\nabla_1 V(1)\,, \tag{12}$$

where use was made of Eq. (11). The first term of Eq. (12) integrates to zero, reflecting the fact that there can be no "self force," and we obtain

$$\mathbf{f} = -Ze\left[\nabla_1 V(1)\right]\big|_{\mathbf{r}_1=\mathbf{R}(t_1)}\,, \tag{13}$$

where we employed

$$\nabla_1^2 U(1) = -4\pi Ze\delta^3(\mathbf{r}_1-\mathbf{R}(t_1))\,. \tag{14}$$

Substitution of $V(1)$ from Eqs. (6) and (11) into Eq. (13) and Fourier transforming both in space and time, we find

$$\begin{aligned}\mathbf{f} \;=\; & -4\pi\,(Ze)^2\left(\nabla_1\left(\int dz_2\int\frac{d^2\bar{\mathbf{p}}}{(2\pi)^2}e^{i\bar{\mathbf{p}}\cdot\bar{\mathbf{r}}_1}\right.\right.\\ & \left.\left.\times\int\frac{dp_z}{2\pi}e^{ip_z z_2}e^{-i(\bar{\mathbf{p}}\cdot\bar{\mathbf{v}}+p_z v_z)t_1}e^{-i\left(\bar{\mathbf{p}}\cdot\bar{\mathbf{R}}_0+p_z z_0\right)}\frac{K(z_1,z_2,\bar{\mathbf{p}};\omega=\bar{\mathbf{p}}\cdot\bar{\mathbf{v}}+p_z v_z)}{\bar{p}^2+p_z^2}\right)\right)\Bigg|_{\mathbf{r}_1=\mathbf{v}t_1+\mathbf{R}_0},\end{aligned} \tag{15}$$

where $\mathbf{v}=\bar{\mathbf{v}}+v_z\hat{\mathbf{z}}$, $\mathbf{r}=(\bar{\mathbf{r}},z)$, and $\mathbf{p}=(\bar{\mathbf{p}},p_z)$. Writing the force as $\mathbf{f}=\bar{\mathbf{f}}+f_z\hat{\mathbf{z}}$, we obtain for the force component perpendicular to the graphene sheet,

$$f_z = -4\pi\,(Ze)^2\int dz_2\int\frac{d^2\bar{\mathbf{p}}}{(2\pi)^2}\int\frac{dp_z}{2\pi}\frac{e^{ip_z(z_2-v_z t_1-z_0)}}{\bar{p}^2+p_z^2}\left(\frac{\partial}{\partial z_1}K(z_1,z_2,\bar{\mathbf{p}};\omega=\bar{\mathbf{p}}\cdot\bar{\mathbf{v}}+p_z v_z)\right)\Bigg|_{z_1=v_z t_1+z_0}. \tag{16}$$

Considering charged particle motion perpendicular to the graphene sheet, $\bar{\mathbf{v}}=0$, and the resistive force of Eq. (16) reduces to

$$f_z = -4\pi\,(Ze)^2\int dz_2\int\frac{d^2\bar{\mathbf{p}}}{(2\pi)^2}\int_{-\infty}^{\infty}\frac{dp_z}{2\pi}\frac{e^{ip_z(z_2-v_z t_1-z_0)}}{\bar{p}^2+p_z^2}\frac{\partial}{\partial z_0}K(v_z t_1+z_0,z_2,\bar{\mathbf{p}};\omega=p_z v_z)\,, \tag{17}$$

where $\bar{p}=|\bar{\mathbf{p}}|$. The quantity of interest here is the total work integral

$$W = \int_{-\infty}^{\infty} dz_0\, f_z, \tag{18}$$

which may be evaluated by integration by parts as

$$W = 4\pi\,(Ze)^2\int dz_2\int d\tilde{z}_0\int\frac{d^2\bar{\mathbf{p}}}{(2\pi)^2}\int_{-\infty}^{\infty}\frac{dp_z}{2\pi}e^{ip_z(z_2-\tilde{z}_0)}\frac{p_z}{\bar{p}^2+p_z^2}K_2(\tilde{z}_0,z_2,\bar{\mathbf{p}};\omega=p_z v_z)\,, \tag{19}$$

with $\tilde{z}_0 = z_0+v_z t_1$, and we wrote $K=K_1+iK_2$ where K_1 (K_2) represents the real (imaginary) part of K. The inverse dielectric function $K(z_1,z_2,\bar{\mathbf{p}};\omega)$ for a $2D$ plasma sheet in $3D$ space is determined as

$$K(z_1,z_2,\bar{\mathbf{p}};\omega) = \frac{1}{\kappa}\delta(z_1-z_2)+\frac{1}{\kappa}\delta(z_2)\,e^{-\bar{p}|z_1|}\left[K^{2D}(\bar{\mathbf{p}},\omega)-1\right], \tag{20}$$

where $K^{2D}(\bar{\mathbf{p}},\omega)$ is the $2D$ inverse dielectric function on the $2D$ plane. Substitution of Eq. (20) into Eq. (19) and evaluation of the $\tilde{z}_0$-integral yields the total work integral as

$$W = \frac{4\pi}{\kappa}\,(Ze)^2\int\frac{d^2\bar{\mathbf{p}}}{(2\pi)^2}\int_{-\infty}^{\infty}\frac{dp_z}{2\pi}\frac{2p_z\bar{p}}{(\bar{p}^2+p_z^2)^2}K_2^{2D}(\bar{\mathbf{p}},\omega=p_z v_z)\,. \tag{21}$$

2. Low Velocity Limit

The screening function may be written in terms of the real and imaginary parts as

$$K^{2D}(\bar{\mathbf{p}},\omega)=\frac{1}{1+\alpha(\bar{\mathbf{p}},\omega)}=\frac{\varepsilon_1(\bar{\mathbf{p}},\omega)-i\alpha_2(\bar{\mathbf{p}},\omega)}{\varepsilon_1^2(\bar{\mathbf{p}},\omega)+\alpha_2^2(\bar{\mathbf{p}},\omega)}. \tag{22}$$

The zero-temperature polarizability for doped/gated graphene ($E_F\neq 0$) was determined [1–5] explicitly in the degenerate case, and the result is written below in terms of the density perturbation response function, R (expressed in terms of the dimensionless quantities $x=\bar{p}/k_F$, $\nu=\omega/E_F$, and $\tilde{R}(\bar{p},\omega)=R(\bar{p},\omega)/D_0$, where $D_0\equiv D(E_F)=\left(g_s g_v n/\pi\right)^{1/2}/\gamma$ is the density of states at the Fermi energy, γ is essentially the $2D$ Fermi velocity, g_s and g_v are the spin and valley degeneracies respectively, and we take $\hbar=1$ and $\alpha_0=0$):

$$\tilde{R}(x,\nu)=\tilde{R}^{+}(x,\nu)+\tilde{R}^{-}(x,\nu)\,, \tag{23}$$

with

$$\tilde{R}^{+}(x,\nu)=\tilde{R}_1^{+}(x,\nu)\,\theta(\nu-x)+\tilde{R}_2^{+}(x,\nu)\,\theta(x-\nu)\,, \tag{24}$$

where the real parts of the polarizability are

$$\begin{aligned}\Re\tilde{R}_1^{+}(x,\nu) &= -1+\tfrac{1}{8\sqrt{\nu^2-x^2}}\Big\{f_1(x,\nu)\,\theta(|2+\nu|-x)+\mathrm{sgn}(\nu-2+x)\,f_1(x,-\nu)\,\theta(|2-\nu|-x)\\ &\qquad +f_2(x,\nu)\left[\theta(x+2-\nu)+\theta(2-x-\nu)\right]\Big\},\end{aligned} \tag{25}$$

$$\begin{aligned}\Re\tilde{R}_2^{+}(x,\nu) &= -1+\tfrac{1}{8\sqrt{x^2-\nu^2}}\Big\{f_3(x,\nu)\,\theta(x-|\nu+2|)+f_3(x,-\nu)\,\theta(x-|\nu-2|)\\ &\qquad +\tfrac{\pi x^2}{2}\left[\theta(|\nu+2|-x)+\theta(|\nu-2|-x)\right]\Big\},\end{aligned} \tag{26}$$

and the imaginary parts of the polarizability are

$$\Im\tilde{R}_1^{+}(x,\nu)=\frac{1}{8\sqrt{\nu^2-x^2}}\Big\{f_3(x,-\nu)\,\theta(x-|\nu-2|)+\frac{\pi x^2}{2}\left[\theta(x+2-\nu)+\theta(2-x-\nu)\right]\Big\}, \tag{27}$$

$$\Im\tilde{R}_2^{+}(x,\nu)=-\frac{\theta(\nu-x+2)}{8\sqrt{x^2-\nu^2}}\left[f_4(x,\nu)-f_4(x,-\nu)\,\theta(2-x-\nu)\right], \tag{28}$$

where

$$f_1(x,\nu)=(2+\nu)\sqrt{(2+\nu)^2-x^2}-x^2\ln\frac{\sqrt{(2+\nu)^2-x^2}+(2+\nu)}{\left|\sqrt{\nu^2-x^2}+\nu\right|}, \tag{29}$$

$$f_2(x,\nu)=x^2\ln\frac{\nu-\sqrt{\nu^2-x^2}}{x}, \tag{30}$$

$$f_3(x,\nu)=(2+\nu)\sqrt{x^2-(2+\nu)^2}+x^2\sin^{-1}\frac{2+\nu}{x}, \tag{31}$$

$$f_4(x,\nu) = (2+\nu)\sqrt{(2+\nu)^2 - x^2} - x^2 \ln \frac{\sqrt{(2+\nu)^2 - x^2} + (2+\nu)}{x}, \tag{32}$$

and

$$\tilde{R}^-(x,\nu) = -\frac{\pi x^2 \theta(x-\nu)}{8\sqrt{x^2-\nu^2}} - i\frac{\pi x^2 \theta(\nu - x)}{8\sqrt{\nu^2 - x^2}}. \tag{33}$$

In the low velocity limit we expand the imaginary part of the inverse dielectric function, $K_2^{2D}(\bar{\mathbf{p}},\omega)$, to linear order in $\omega = p_z v_z$, obtaining

$$K_2^{2D}(\bar{\mathbf{p}},\omega) \simeq K_2^{2D}(\bar{\mathbf{p}},0) + \omega \left(\frac{\partial}{\partial\omega} K_2^{2D}(\bar{\mathbf{p}},\omega)\right)\Big|_{\omega=0} = \omega \left(\frac{\partial}{\partial\omega} K_2^{2D}(\bar{\mathbf{p}},\omega)\right)\Big|_{\omega=0}, \tag{34}$$

since $K_2^{2D}(\bar{\mathbf{p}},\omega)$ is an odd function of frequency ω. Using Eq. (22), we write Eq. (34) as

$$K_2^{2D}(\bar{\mathbf{p}},\omega) \simeq \omega \frac{v_c(\bar{p})\,\frac{\partial}{\partial\omega} R_2(\bar{\mathbf{p}},\omega=0)}{\left[1 - v_c(\bar{p})\,R_1(\mathbf{p},0)\right]^2}, \tag{35}$$

and substitution into Eq. (21) yields the total work integral as

$$|W| = -4\pi^2 v_z \left(\frac{Ze^2}{\kappa}\right)^2 \int \frac{d^2\bar{\mathbf{p}}}{(2\pi)^2} \frac{1}{\bar{p}} \frac{\frac{\partial}{\partial\omega} R_2(\bar{\mathbf{p}},\omega=0)}{\left[1 - v_c(\bar{p})\,R_1(\mathbf{p},0)\right]^2}, \tag{36}$$

which, in terms of the dimensionless variables introduced above, can be recast as

$$|W| = -2\pi v_z \frac{D_0 p_F}{E_F} \left(\frac{Ze^2}{\kappa}\right)^2 \int_0^\infty dx \frac{\frac{\partial}{\partial\nu}\tilde{R}_2(x,\nu=0)}{\left[1 - \frac{2\pi e^2 D_0}{\kappa p_F}\frac{1}{x}\tilde{R}_1(x,\nu=0)\right]^2}. \tag{37}$$

The expressions appearing in the above integrand are

$$\frac{\partial}{\partial\nu}\tilde{R}_2(x,\nu=0) = -\frac{1}{2x}\sqrt{4-x^2}\,\theta(2-x)\,\theta(x)\,, \tag{38}$$

and

$$\tilde{R}_1(x,\nu=0) = -1 - \frac{\pi x}{8}\theta(x-2) + \frac{1}{4x}\left(2\sqrt{x^2-4} + x^2 \sin^{-1}\left(\frac{2}{x}\right)\right)\theta(x-2)\,. \tag{39}$$

Substitution of the above two expressions into Eq. (37) yields

$$|W| = \pi v_z \frac{D_0 p_F}{E_F} \left(\frac{Ze^2}{\kappa}\right)^2 \int_0^2 dx \frac{x\sqrt{4-x^2}}{(x+c)^2}, \tag{40}$$

where we have defined $c = 2\pi e^2 D_0/\kappa p_F$. Executing the x-integral we obtain the following expression for the total work integral

$$|W| = \pi v_z \frac{D_0 p_F}{E_F} \left(\frac{Ze^2}{\kappa}\right)^2 \left[c\pi - 4 - \frac{2\,(c^2-2)}{\sqrt{c^2-4}} \cos^{-1}\left(\frac{2}{c}\right)\right]. \tag{41}$$

3. High Velocity Limit

In the case of a high velocity probe particle the principal contribution to energy loss arises from the excitation of plasmons and consequently the denominator on the right side of Eq. (22) must vanish and can not be subjected to any contrary approximation. However, there is simplification due to the fact that the frequency argument at high velocity, $\omega = p_z v_z$ dominates, driving the polarizability into its local limit. Thus, in the high velocity case

$$K^{2D}\left(\bar{\mathbf{p}},\omega\right) \to K^{2D}(0,\omega) = \frac{1}{\varepsilon^{2D}(0,\omega)}, \tag{42}$$

with $\varepsilon^{2D}\left(0,\omega\right)$ the high frequency local dielectric function, which has the same structure for graphene as it does for electrons with parabolic dispersion:

$$\varepsilon^{2D}(0,\omega) = 1 - \frac{\omega_p^2}{\omega^2}, \tag{43}$$

where $\omega_p = \left(\gamma e^2\sqrt{n\pi g_s g_v}/\kappa\hbar\right)^{1/2}\sqrt{\bar{p}} \equiv \lambda\sqrt{\bar{p}}$ is the graphene plasma frequency [4]. The imaginary part of the inverse dielectric function is obtained by letting $\omega \to \omega + i0^+$ (with 0^+ a positive infinitesimal) in Eq. (43), resulting in $K_2(\mathbf{p},\omega) = -\frac{\pi\omega_p}{2}\left(\delta\left(\omega-\omega_p\right) - \delta\left(\omega+\omega_p\right)\right)$. The total work integral of Eq. (21) may be written using this form of $K_2(\mathbf{p},\omega)$ for high velocity as

$$\begin{aligned} W &= -\frac{4\pi}{\kappa}\left(Ze\right)^2 \int \frac{d^2\bar{\mathbf{p}}}{\left(2\pi\right)^2}\int_0^\infty dp_z \frac{p_z\bar{p}}{\left(\bar{p}^2+p_z^2\right)^2}\frac{\omega_p}{v_z}\delta\left(p_z - \frac{\omega_p}{v_z}\right) \\ &= -\frac{4\pi}{\kappa}\left(Ze\frac{\lambda}{v_z}\right)^2 \int_0^\infty \frac{d\bar{p}}{2\pi}\frac{\bar{p}^3}{\left(\bar{p}^2+\bar{p}\left(\frac{\lambda}{v_z}\right)^2\right)^2}. \end{aligned} \tag{44}$$

Finally we employ an upper upper cutoff p_c for the $\bar{p}$-integral, with p_c marking the maximum momentum for which the plasmon approximation is valid, namely $\gamma p < \omega < 2E_F$ or $p^{1/2} < \lambda/v_F$. The resulting total work in the perpendicular case is given by

$$W = \frac{2}{\kappa}\left(Ze\frac{\lambda}{v_z}\right)^2\left(\frac{v_z^2}{v_z^2+v_F^2} - \ln\left(1+\frac{v_z^2}{v_F^2}\right)\right). \tag{45}$$

In Fig. 1 we plot the total work $|W|$ (in units of $(Ze\lambda/v_z)^2/\kappa$) as a function of v_z (in units of v_F) in the high velocity limit. It is important to note that while the high velocity result in the plasmon approximation closely resembles that of a normal plasma with a quadratic dispersion law, the case of graphene substantially differs in regard to density dependence because $\omega_p = \left(g_s g_v e^2 E_F/2\kappa\hbar^2\right)^{1/2}\sqrt{\bar{p}} = \left(\gamma e^2\sqrt{n g_s g_v}/\kappa\hbar\right)^{1/2}\sqrt{\bar{p}}$, wherein the Fermi velocity, γ, is independent of density and the Fermi energy involves density in the form $E_F = \gamma p_F = \gamma\left(4\pi n/g_s g_v\right)^{1/2}$, leading to $\omega_p \propto n^{1/4}$ instead of the usual $n^{1/2}$.

In conclusion, we have presented explicit expressions for the energy loss of a fast charged particle moving perpendicular to a two-dimensional graphene sheet. In particular, we have considered both the low and high velocity limits and have stated the differences between the normal two-dimensional plasma results and those in the presence of graphene.

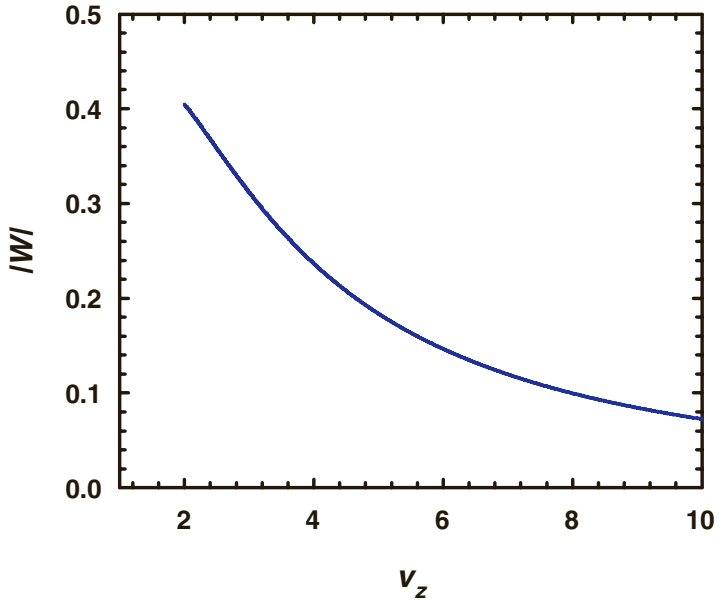

Figure 1. Plot of $|W|$ (in units of $(Ze\lambda/v_z)^2/\kappa$) as a function of v_z (in units of v_F) in the high velocity limit.

REFERENCES

1. K.W.-K. Shung, Phys. Rev. B 34 (1986) 979.
2. K.W.-K. Shung, Phys. Rev. B 34 (1986) 1264.
3. T. Ando, J. Phys. Soc. Jpn. 75 (2006) 074716.
4. E.H. Hwang and S. Das Sarma, Phys. Rev. B 75 (2007) 205418.
5. B. Wunsch, T. Stauber, F. Sols and F. Guinea, New J. Phys. 8 (2006) 318.